

## THE BIGGEST EXPLOSIONS IN THE UNIVERSE. II.

DANIEL J. WHALEN<sup>1,2</sup>, JARRETT L. JOHNSON<sup>3</sup>, JOSEPH SMIDT<sup>1</sup>, ALEXANDER HEGER<sup>4</sup>, WESLEY EVEN<sup>5</sup> AND CHRIS L. FRYER<sup>5</sup>

*Draft version September 25, 2018*

### ABSTRACT

One of the leading contenders for the origin of supermassive black holes at  $z \gtrsim 7$  is catastrophic baryon collapse in atomically-cooled halos at  $z \sim 15$ . In this scenario, a few protogalaxies form in the presence of strong Lyman-Werner UV backgrounds that quench H<sub>2</sub> formation in their constituent halos, preventing them from forming stars or blowing heavy elements into the intergalactic medium prior to formation. At masses of  $10^8 M_{\odot}$  and virial temperatures of  $10^4$  K, gas in these halos rapidly cools by H lines, in some cases forming  $10^4 - 10^6 M_{\odot}$  Pop III stars and, a short time later, the seeds of supermassive black holes. Instead of collapsing directly to black holes some of these stars died in the most energetic thermonuclear explosions in the universe. We have modeled the explosions of such stars in the dense cores of line-cooled protogalaxies in the presence of cosmological flows. In stark contrast to the explosions in diffuse regions in previous simulations, these SNe briefly engulf the protogalaxy but then collapse back into its dark matter potential. fallback drives turbulence that efficiently distributes metals throughout the interior of the halo and fuels the rapid growth of nascent black holes at its center. The accompanying starburst and x-ray emission from these line-cooled galaxies easily distinguish them from more slowly evolving neighbors and might reveal the birthplaces of supermassive black holes on the sky.

*Subject headings:* early universe – galaxies: high-redshift – galaxies: quasars: general – stars: early-type – supernovae: general – radiative transfer – hydrodynamics – black hole physics – accretion – cosmology:theory

### 1. INTRODUCTION

The existence of supermassive black holes (SMBHs) in galaxies at  $z \gtrsim 7$  (Fan et al. 2003; Willott et al. 2003; Fan et al. 2006; Mortlock et al. 2011) poses one of the greatest challenges to the paradigm of hierarchical structure formation (Bromm & Loeb 2003; Begelman et al. 2006; Johnson & Bromm 2007; Djorgovski et al. 2008; Lippai et al. 2009; Tanaka & Haiman 2009; Pan et al. 2012b; Schleicher et al. 2013; Choi et al. 2013). One of the leading contenders for the origin of SMBHs is catastrophic baryon collapse in atomically cooled halos at  $z \sim 10 - 15$  (Wise et al. 2008; Regan & Haehnelt 2009; Shang et al. 2010; Wolcott-Green et al. 2011; Latif et al. 2013a,b). In this picture, a few primeval galaxies (Johnson et al. 2008; Greif et al. 2008; Johnson et al. 2009; Greif et al. 2010; Jeon et al. 2012; Pawlik et al. 2011; Wise et al. 2012; Pawlik et al. 2013) formed in strong Lyman-Werner (LW) UV backgrounds that photodissociated all their H<sub>2</sub>, preventing them from forming primordial stars prior to assembly (Bromm et al. 1999; Abel et al. 2000, 2002; Bromm et al. 2002; Nakamura & Umemura 2001; O’Shea & Norman 2007, 2008; Wise & Abel 2007; Yoshida et al. 2008;

Turk et al. 2009; Stacy et al. 2010; Smith et al. 2011; Clark et al. 2011; Greif et al. 2011; Hosokawa et al. 2011; Greif et al. 2012; Susa 2013). Unlike other primitive galaxies, which began to reionize (Whalen et al. 2004; Kitayama et al. 2004; Alvarez et al. 2006; Abel et al. 2007; Wise & Abel 2008) and chemically enrich the IGM (Mackey et al. 2003; Smith & Sigurdsson 2007; Smith et al. 2009; Joggerst et al. 2010; Joggerst & Whalen 2011; Ritter et al. 2012; Chiaki et al. 2013; Safranek-Shrader et al. 2013), line-cooled protogalaxies remained inert until reaching masses of  $\sim 10^8 M_{\odot}$  and virial temperatures of  $\sim 10^4$  K.

These temperatures activated rapid cooling in the halo by H lines, triggering massive baryon collapse with central infall rates of up to  $0.1 - 1 M_{\odot} \text{ yr}^{-1}$ , 1000 times those that formed the first stars in less massive halos at higher redshifts. Such accretion rates were capable of building up very massive gas clumps in short times, most of which collapsed directly to  $10^4 - 10^5 M_{\odot}$  BHs. The creation of SMBH seeds by direct baryon collapse has gained ground in recent years because it has been shown that Population III (Pop III) BH seeds cannot achieve the rapid growth needed to reach  $10^9 M_{\odot}$  by  $z \sim 7$  (Milosavljević et al. 2009; Alvarez et al. 2009; Park & Ricotti 2011; Mortlock et al. 2011; Park & Ricotti 2012; Whalen & Fryer 2012; Park & Ricotti 2013; Johnson et al. 2013b). It was originally thought that LW fluxes capable of fully suppressing Pop III star formation were rare, and that this might explain why so few SMBHs have been found at  $z \gtrsim 6$ , but it is now known that such environments may have been far more common in the early universe than previ-

<sup>1</sup> T-2, Los Alamos National Laboratory, Los Alamos, NM 87545

<sup>2</sup> Universität Heidelberg, Zentrum für Astronomie, Institut für Theoretische Astrophysik, Albert-Ueberle-Str. 2, 69120 Heidelberg, Germany

<sup>3</sup> XTD-6, Los Alamos National Laboratory, Los Alamos, NM 87545

<sup>4</sup> Monash Centre for Astrophysics, Monash University, Victoria, 3800, Australia

<sup>5</sup> CCS-2, Los Alamos National Laboratory, Los Alamos, NM 87545

ously believed (Dijkstra et al. 2008; Johnson et al. 2012; Agarwal et al. 2012; Petri et al. 2012).

In some cases, massive clumps in line-cooled halos formed stable stars rather than collapsing directly to BHs (Iben 1963; Fowler & Hoyle 1964; Fowler 1966; Appenzeller & Fricke 1972a,b; Bond et al. 1984; Fuller et al. 1986; Begelman 2010). Some of these stars have now been shown to die in extremely energetic thermonuclear explosions (Montero et al. 2012; Heger & Chen 2013) that will be visible in both deep-field and all-sky NIR surveys at  $z \gtrsim 10$  by the *James Webb Space Telescope (JWST)*, *Euclid*, the Wide-Field Infrared Survey Telescope (WFIRST), and the Wide-Field Imaging Surveyor for High-Redshift (WISH) (Whalen et al. 2012b) (for other work on Pop III SN light curves, see Scannapieco et al. 2005; Fryer et al. 2010; Kasen et al. 2011; Pan et al. 2012a; Hummel et al. 2012; Dessart et al. 2013; Whalen et al. 2013b; Meiksin & Whalen 2013; Whalen et al. 2012a, 2013c,a; de Souza et al. 2013). A  $55,500 M_{\odot}$  SN in a diffuse environment in its host protogalaxy has been studied by Johnson et al. (2013a). For explosions in low densities, like those of an H II region created by the star, they find that the SN expels all the baryons from the halo to radii of  $\gtrsim 10$  kpc. In this scenario, metals from the SN can enrich nearby protogalaxies before later falling back into the halo on timescales of 50 - 70 Myr.

If the explosion instead occurs in the heavy infall that formed the star, the SN rapidly loses energy to bremsstrahlung and line emission and expands to at most 1 kpc, the virial radius of the halo (Whalen et al. 2013d) (see also Kitayama & Yoshida 2005; Whalen et al. 2008; de Souza et al. 2011; Vasiliev et al. 2012). Ejecta from the SN briefly displaces the outer layers of the protogalaxy but then recollapses in a spectacular bout of fallback that was inferred to rapidly distribute heavy elements throughout its interior and fuel the growth of massive SMBH seeds at its center. However, the extremely short X-ray and line cooling timescales in the dense media plowed up by the SN limited these simulations to one dimension (1D), so they could not follow the evolution of the protogalaxy during expansion and fallback or determine how cosmological flows later mixed its interior with metals.

However, it is possible to initialize a three-dimensional (3D) cosmological simulation with 1D blast profiles from Whalen et al. (2013d) at intermediate times, after cooling timescales in the shock have become large but before it has reached large radii or departed from spherical symmetry. The explosion can then be evolved in the protogalaxy in the presence of cosmological flows to determine its eventual fate, having properly determined its energy and momentum losses over all spatial scales. We have now performed such a simulation in the GADGET code with a supermassive SN profile taken from the ZEUS-MP calculations of Whalen et al. (2013d). We describe our numerical simulation in Section 2. The evolution of the SN in the presence of cosmological flows is examined in Section 3, where we also study the metallicity of the halo over time. We then discuss the potential for triggered starbursts and rapid central BH growth in the protogalaxy and conclude in Section 4.

## 2. NUMERICAL METHOD

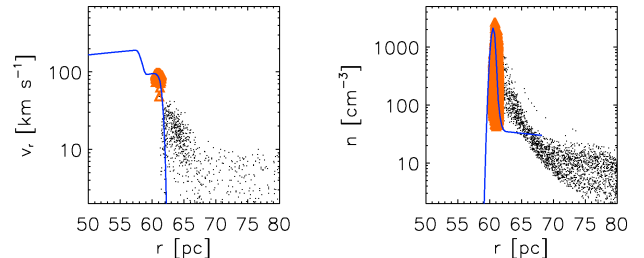


FIG. 1.— GADGET fit to the supermassive SN profiles from ZEUS-MP. Left: radial velocity. Right: number density. The blue curves denote the ZEUS-MP profiles and the orange particles and triangles trace the SPH particle distribution assigned to these profiles. The black points are the SPH particles representing the protogalaxy and cosmological flows.

Our calculation proceeds in three stages. First, the  $55,500 M_{\odot}$  Pop III star is evolved from the beginning of the main sequence to central collapse and then explosion in the *Kepler* (Weaver et al. 1978; Woosley et al. 2002) and RAGE codes (Gittings et al. 2008; Frey et al. 2013), out to  $2.9 \times 10^6$  s. The energy of the SN is  $7.7 \times 10^{54}$  erg. At this time the shock is at  $4 \times 10^{15}$  cm, past breakout from the surface of the star but at a radius at which it has not swept up much mass. The SN is then initialized in ZEUS-MP (Whalen & Norman 2006, 2008a,b) in the spherically averaged 1D profile of the halo into which it is later mapped in GADGET. The density of the halo at the radius of the shock is  $\sim 10^{11} \text{ cm}^{-3}$  (see Fig. 3 of Whalen et al. 2013d). The SN is evolved out to 60 pc (at  $2.54 \times 10^5$  yr) and then both it and the gas it has swept up are ported to GADGET. These first two steps are described in detail in Whalen et al. (2012b) and Whalen et al. (2013d).

In Johnson et al. (2013a) the SN was initialized in a diffuse  $r^{-2}$  wind envelope whose density was far lower than that of the undisturbed halo in ZEUS-MP (see Fig. 3 of Whalen et al. 2012b). This wind approximated an H II region created by the star. The SN was evolved out to 6 pc in RAGE and then mapped into the center of the protogalaxy in GADGET. Our procedure ensures that the heavy energy losses of the SN in a dense protogalactic core are properly taken into account, and that the explosion is initialized with the proper energy and momentum in our cosmological simulation.

### 2.1. GADGET Model

Our fiducial protogalaxy is the  $4 \times 10^7 M_{\odot}$  atomically-cooled halo from Johnson et al. (2013a), which forms in a  $1 \text{ Mpc}^3$  (comoving) simulation volume in GADGET (Springel et al. 2001; Springel & Hernquist 2002). This simulation was evolved from  $z = 100$  down to  $z \sim 15$  in a uniform LW UV background that sterilized the halo of  $\text{H}_2$  and prevented stars from forming in any of its constituent halos. The simulation that produced the protogalaxy is described in Johnson et al. (2011). We map the (Eulerian) ZEUS-MP SN profile into the (Lagrangian) smoothed-particle hydrodynamics (SPH) GADGET model by assigning the central 11,373 SPH particles to the ejecta in a manner that reproduces the radial velocity and number density of the blast. We show our fit to the ZEUS-MP profile in Fig. 1. The SN

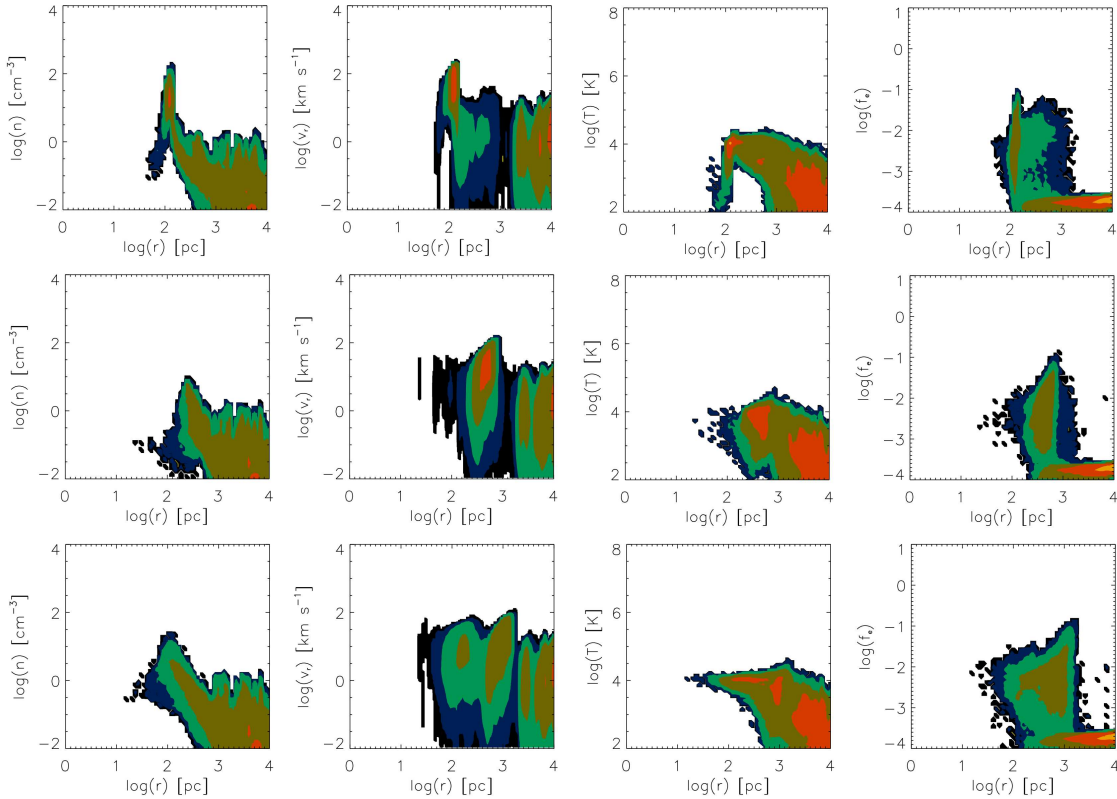


FIG. 2.— Protogalactic baryons plowed up by the supermassive SN at 1 Myr (*top*), 10 Myr (*center*) and 25 Myr (*bottom*). Left to right: H number density, radial gas velocity, temperature and free electron fraction, all as a function of radius from the center of the halo. Mass fractions in the gas change by an order of magnitude across the contours in the plots.

expels 23,000  $M_{\odot}$  of metals (and probably molecules and dust; Cherchneff & Lilly 2008; Cherchneff & Dwek 2009, 2010; Dwek & Cherchneff 2011; Gall et al. 2011) into the galaxy. At this stage it is essentially a free expansion.

We initialize the shock at 60 pc in GADGET for two reasons. First, the shock must expand and cool to temperatures at which its chemistry and cooling times are long enough to evolve it in a 3D cosmological simulation in a reasonable time. It cannot be initialized with too large a radius because our GADGET simulation might then exclude asymmetries that can arise in the shock at earlier times. We found that 60 pc (in contrast to 6 pc in Johnson et al. 2013a) satisfied both requirements. This radius was also chosen to minimize departures from mass conservation when assigning the SPH particle distribution to the high-resolution ZEUS-MP SN profile. There was a fair amount of ejecta and swept-up gas in ZEUS-MP at radii below what could have been resolved by our GADGET model at early times. Allowing the SN to grow to  $\sim 60$  pc in ZEUS-MP enabled us to preserve its mass to within 20% in GADGET. Smaller errors could have been achieved with larger radii but at the cost of missing asymmetries in the shock due to inhomogeneities in the cosmological density field. We obtained even better agreement in mass conservation at just 6 pc in Johnson et al. (2013a) because the explosion was in lower densities that could be adequately resolved at smaller radii by the SPH particle distribution.

## 2.2. Nonequilibrium H/He Gas Chemistry

We evolve mass fractions for H, H<sup>+</sup>, He, He<sup>+</sup>, He<sup>++</sup>, H<sup>-</sup>, H<sub>2</sub><sup>+</sup>, H<sub>2</sub>, e<sup>-</sup>, D, D<sup>+</sup> and HD with the 42 reaction rate network described in Johnson & Bromm (2006) to tally energy losses in the remnant as it sweeps up and heats baryons. Cooling due to collisional excitation and ionization of H and He, recombinations, inverse Compton (IC) scattering from the cosmic microwave background (CMB), and free-free emission by bremsstrahlung x-rays are included. In the ZEUS-MP run H<sub>2</sub> cooling is turned off in the gas because high temperatures in the shock at early times destroy these fragile molecules. Both H<sub>2</sub> and HD cooling are included in the GADGET run but are minimal because of shock heating and the LW background. Adjustments to LW photodissociation rates due to self-shielding by H<sub>2</sub> and H<sup>-</sup> photodetachment rates are taken from Shang et al. (2010). Cooling times for these processes depend on temperatures and mass fractions for these species in the shocked gas, which in turn are governed by the energy equation and the nonequilibrium reaction network.

## 3. SN EVOLUTION IN THE PROTOGALAXY

### 3.1. Dynamics and Energetics

We show the evolution of gas in the protogalaxy as it is blown outward by the SN at 1, 10 and 25 Myr in Fig. 2. As shown in the center panels on the top row, the shock has cooled to  $\sim 50,000$  K and slowed to  $\sim 300$  km s<sup>-1</sup> by 1 Myr, mostly because of prior energy losses to bremsstrahlung and H and He line emission. Atomic lines restrict the temperature of the shock to

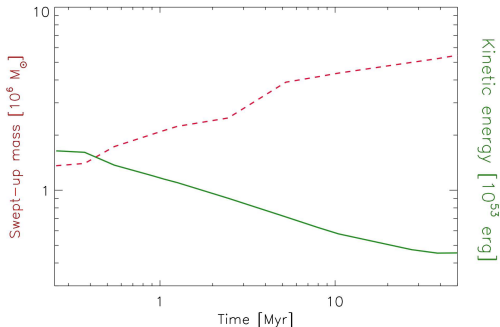


FIG. 3.— The mass swept up by the shock (red dashed line) and the total kinetic energy of the flow (green solid line) as a function of time.

10,000 - 25,000 K thereafter (the "Balmer thermostat"), as in Whalen et al. (2013d). Consequently, free electron fractions never exceed 10%. At 1 Myr there are two components to the electron fraction: collisional ionizations in the SN shock, which are visible as the vertical spike in electron fraction at 100 pc, and ionizations in the virial shock from  $\sim 0.5 - 1$  kpc. The propagation of the shock to the edge of the halo is visible as the red contours in temperature and radial velocity that migrate from 100 pc to 2 kpc over 25 Myr. Similar motion is visible in the spike in electron fraction, which is also at 2 kpc by 25 Myr. The ejecta drives most of the gas from the center of the protogalaxy at early times, as shown in the panels on the left. But the gas then collapses back into the halo sooner than in the Johnson et al. (2013a) run, with fallback approaching the center by  $\sim 25$  Myr. We note that the  $\sim 50 \text{ km s}^{-1}$  gas velocities at radii greater than 500 pc are from cosmological infall and virialization. They are steady throughout the run because accretion continues throughout the simulation.

As shown in Fig. 3, the ejecta has lost 95% of its original kinetic energy by the time it is initialized in GADGET, but, as we show later, it still has enough linear momentum to drive gas in the halo out to its virial radius. Line emission and expansion in the dark matter potential of the halo reduce the kinetic energy to  $4.5 \times 10^{52}$  erg by 25 Myr. The ejecta displaces about the same amount of gas as in the Johnson et al. (2013a) models ( $\sim 10^7 M_{\odot}$ ) but to much smaller radii, 2 kpc rather than 8 - 10 kpc. We show the evolution of the protogalaxy in Fig. 4. Even with blowout into low-density voids, most of the gas is still confined to within  $\sim 2$  kpc of the center of the halo, unlike in Johnson et al. (2013a) in which the ejecta reaches radii of 10 kpc, perhaps enriching nearby halos. As seen in the velocity projections, gas preferentially propagates into the voids but is essentially halted along filaments by cosmological inflows. The SN expands to somewhat larger radii on average in this cosmological simulation than in the ZEUS-MP runs in Whalen et al. (2013d) because of blowout into voids, which cannot be captured in 1D.

One physical process we do not capture in ZEUS-MP or GADGET is the dynamical decoupling of ions from electrons in the shock that may occur 5 - 10 yr after the SN. If these two components do decouple the shock cools less efficiently because the entropy generated by the shock, which is deposited in the ions, cannot be radiated away

efficiently by the electrons. This phenomenon reduces cooling in galactic SN remnants in relatively diffuse ISM densities at intermediate times. Electron-ion decoupling does not affect the explosions of supermassive stars in diffuse regions in line-cooled protogalaxies (Johnson et al. 2013a) because such explosions unbind baryons from the halo anyway. It could allow explosions in the dense regions studied here to grow to larger radii, but it is unclear for how long cooling would be curtailed. Future improvements to RAGE, such as 3-temperature physics in which photons, electrons and ions can be evolved with distinct temperatures, could address these issues. The cooling found in our simulations should therefore be considered to be upper limits for now.

### 3.2. Chemical Enrichment

As with Pop III PI SNe, about half of the mass of the supermassive SN is blown out into the galaxy in the form of heavy elements,  $\sim 23,000 M_{\odot}$ . If the explosion occurs in a dense environment and drives turbulence, these metals can efficiently mix with gas in the halo, enhancing its cooling rates and altering the mass scales on which it fragments and forms new stars (e.g., Bromm et al. 2001; Santoro & Shull 2006; Schneider et al. 2006), even in the presence of strong LW backgrounds (Omukai et al. 2008). We show projections of metallicity at 10, 25 and 50 Myr in Fig. 5. The ejecta bubble is mostly uniform in metallicity when it reaches the virial radius but then some heavy elements continue out into the low-density voids while the rest begin to fall back into the halo. Later, as the collapse of ejecta back into the halo accelerates, inhomogeneities in metallicity become more pronounced. As Fig. 5 shows, metals propagate the least distance along the filaments (at whose intersection the halo originally formed).

We plot the evolution of the metallicity of the halo as a function of radius at 1, 10 and 70 Myr in Fig. 6. By 10 Myr the SN has essentially driven all the metals from the central 50 pc of the halo. But, as shown in the bottom row of Fig. 2, fallback has begun by  $\sim 25$  Myr, raising the metallicity  $Z$  of the protogalaxy to  $0.1 - 0.2 Z_{\odot}$  at  $r \gtrsim 50$  pc compared to  $0.05 - 0.1 Z_{\odot}$  at  $r \gtrsim 100$  pc in Fig. 5 of Johnson et al. (2013a). It is clear that early fallback and the relative confinement of the ejecta in this run drives the interior of the protogalaxy to metallicities that are twice those of the explosions in H II regions in Johnson et al. (2013a). At 70 Myr the entire halo has been enriched to a metallicity  $Z \sim 0.1 Z_{\odot}$  compared to  $Z \sim 0.05 Z_{\odot}$  in Johnson et al. (2013a). There were still a few metal particles less than 50 pc from the center of the halo at 10 Myr whose outward propagation was slowed by strong filamentary inflows along a few lines of sight. These particles are visible as the two spikes in metallicity at radii of  $\lesssim 50$  pc in Fig. 6.

Whalen et al. (2013d) speculated that massive fallback into the halo would not only distribute metals throughout its interior: it, together with cosmological inflows, would also drive turbulence that would efficiently mix the metals with baryons in the protogalaxy and radically alter their cooling properties. However, their 1D models could not simulate these processes. We show the vorticity  $|\nabla \times \vec{v}|$  due to expansion and fallback in a slice through the center of the halo at 50 Myr for this run and Johnson et al. (2013a) in Fig. 7. Vorticity is a measure

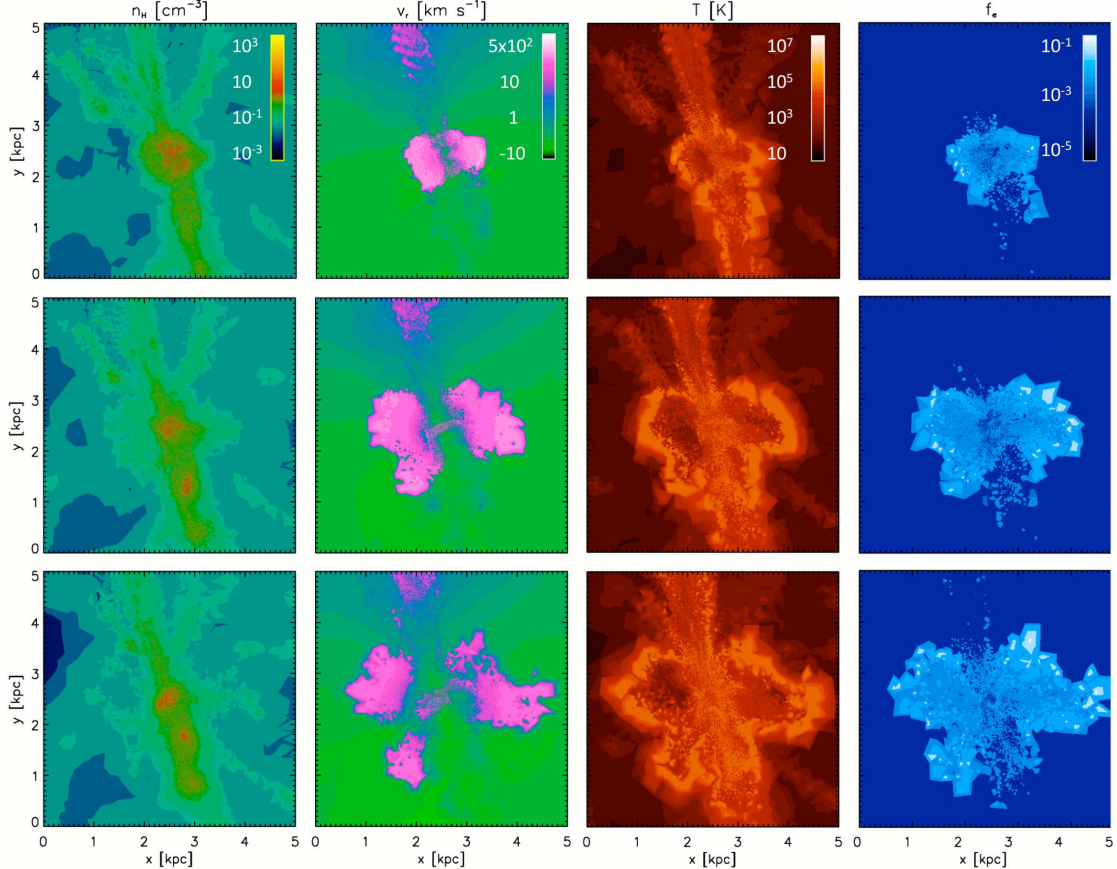


FIG. 4.— The SN at 10 Myr (*top*), 25 Myr (*center*) and 50 Myr (*bottom*). Left to right: projections of H number density, radial gas velocity, temperature and free electron fraction.

of the shear flows that drive Kelvin-Helmholtz instabilities that in turn energize turbulent cascades in the gas. Wherever it is strong, turbulence and efficient mixing are likely to follow. As shown in the bottom row of Fig. 7, both explosions exhibit similar degrees of vorticity, although it is greater at the center of the protogalaxy in the present run where early fallback and accretion collide and churn the gas to a greater degree than in Johnson et al. (2013a). In both cases it is anti-correlated with blowout into low-density voids, which is characterized by rapid expansion without much shear. These flows are marked by the regions of large divergence  $|\nabla \cdot \vec{v}|$  shown in the top row of Fig. 7.

The large vorticities in both explosions suggests that turbulence will enrich most of the baryons in the protogalaxy with metals (and perhaps dust). Star formation and a prompt rollover from a Pop III to a Pop II initial mass function (IMF) may follow throughout the interior of the halo. Although such explosions may be rare events in the early universe, their host galaxies would be easily distinguished from their less rapidly evolving neighbors by their large star formation rates and by their distinct spectral energy distributions (SEDs), which would be almost entirely due to Pop II stars.

### 3.3. Fallback and SMBH Seed Growth

Outflow and fallback through a spherical boundary at 1 kpc, the virial radius of the halo, are shown for this

run and for Johnson et al. (2013a) in Fig. 8. Differences in the overall dynamics between SNe in dense accretion envelopes and diffuse H II regions are abundantly clear. First, blowout happens sooner in low density environments than in heavy infall, in which the shock does not reach the virial radius and reverse accretion onto the halo until  $\sim 10$  Myr. Peak outflow rates are also much higher in Johnson et al. (2013a) due to lower energy losses and breakout into low density voids. Fallback is heavier in our run at late times because little of the ejecta is unbound from the halo, unlike Johnson et al. (2013a) in which metals blown out into voids only return after a fraction of a Hubble time. It might be thought from the relative positions of the two peaks in outflow that fallback begins earlier in Johnson et al. (2013a) than in this run. In reality, as noted above, fallback begins earlier in explosions in dense regions. In these cases much of the ejecta never reaches 1 kpc and does not appear in the plot. These metals fall back to the center of the halo well before ejecta in explosions in low densities returns to the halo (compare Fig. 2 in this study to Fig. 2 in Johnson et al. 2013a).

Steady cosmological inflow from filaments is evident in the present run until  $\sim 10$  Myr, after which the SN reverses them. Comparing this plot to Figs. 6 and 7b in Whalen et al. (2013d), it is clear that cosmological flows somewhat dampen the massive fallback of 1D models, averaging them out over time. This happens in part be-

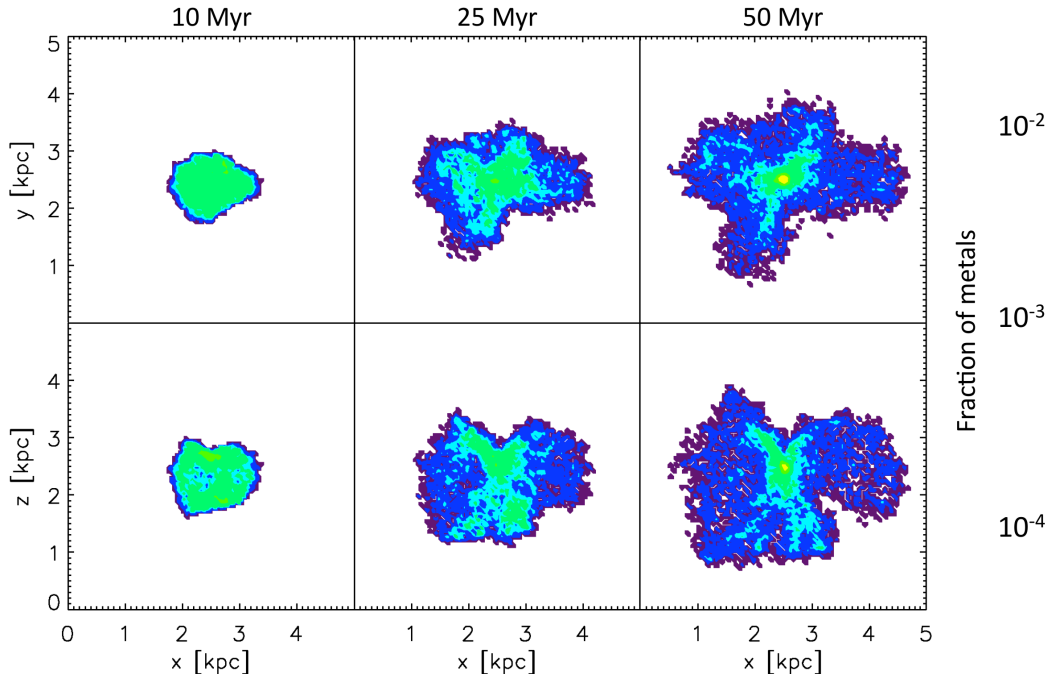


FIG. 5.— Projections of metallicity along the  $y$ - (*top*) and the  $z$ -axes (*bottom*) at 10 Myr (*left*), 25 Myr (*center*) and 50 Myr (*right*).

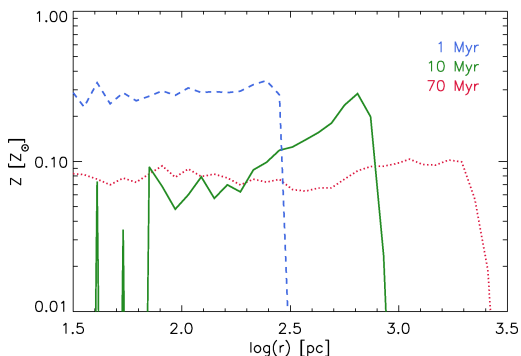


FIG. 6.— Spherical average of the metallicity  $Z$  of the gas (in units of solar metallicity  $Z_{\odot}$ ) as a function of radius at 1 Myr (*blue dashed line*), 10 Myr (*green solid line*) and 70 Myr (*red dotted line*).

cause metals along some lines of sight fall back into the halo sooner as they encounter inflow along dense filaments. As shown in the left panels of Fig. 7, accretion and fallback also drive turbulent motions in the halo that partially support the gas against collapse. However, fallback eventually drives central accretion rates to values greater than those originally due to filaments alone, as shown in the slope of the red plot after 55 Myr.

Fallback in both explosions eventually results in flows capable of rapidly growing SMBH seeds at the center of the protogalaxy. How x-rays from nascent black holes regulate these infall rates ( $\gtrsim 0.04 M_{\odot} \text{ yr}^{-1}$ ) remains to be determined. Nevertheless, it is probable that baryon collapse rates of this magnitude could drive episodes of super-Eddington accretion by central BHs. We note that fragmentation of the atomically-cooled disk at the center of the halo almost certainly leads to multiple supermas-

sive clumps (see Fig. 1 of Whalen et al. 2012b). Supermassive stars and SMBH seeds therefore probably coexist at the center of the protogalaxy, and massive BHs would remain after the explosion of one of the stars.

#### 4. DISCUSSION AND CONCLUSION

In Johnson et al. (2013a) and this paper, we have considered the two extremes for supermassive Pop III SNe in line-cooled protogalaxies: explosions in diffuse regions, like an H II region of the star, and explosions in dense envelopes, like those that gave birth to the star. We find that SNe in dense protogalactic cores do not grow to radii much larger than that of the halo, unlike explosions in low-density regions whose metals can envelop and enrich nearby galaxies. In reality, explosions of supermassive Pop III stars occur in regions that fall somewhere in between these two extremes, depending on the rates and geometry of accretion and whether or not ionizing UV radiation from the progenitor breaks out of its accretion envelope (Johnson et al. 2012). These spectacular events are likely accompanied by intense starbursts and rapid growth of SMBH seeds driven by massive fallback and prompt chemical enrichment of baryons in the halo.

Supermassive Pop III SNe can be detected on multiple, disparate timescales after they occur, beginning with the prompt NIR emission from the initial blast. Whalen et al. (2012b) find that explosions in dense envelopes are much brighter in the NIR than SNe in diffuse regions and can be detected at  $z \sim 15 - 20$  by WFIRST, WISH and *JWST* and at  $z \sim 10 - 15$  by *Euclid*. This point is important because all-sky surveys by missions such as WFIRST, WISH and *Euclid* could discover these explosions in spite of their small numbers. Later, on timescales of  $\sim 10^3$  yr, the SN remnant becomes a strong synchrotron source that is visible in the radio to eVLA, eMERLIN, ASKAP and the Square

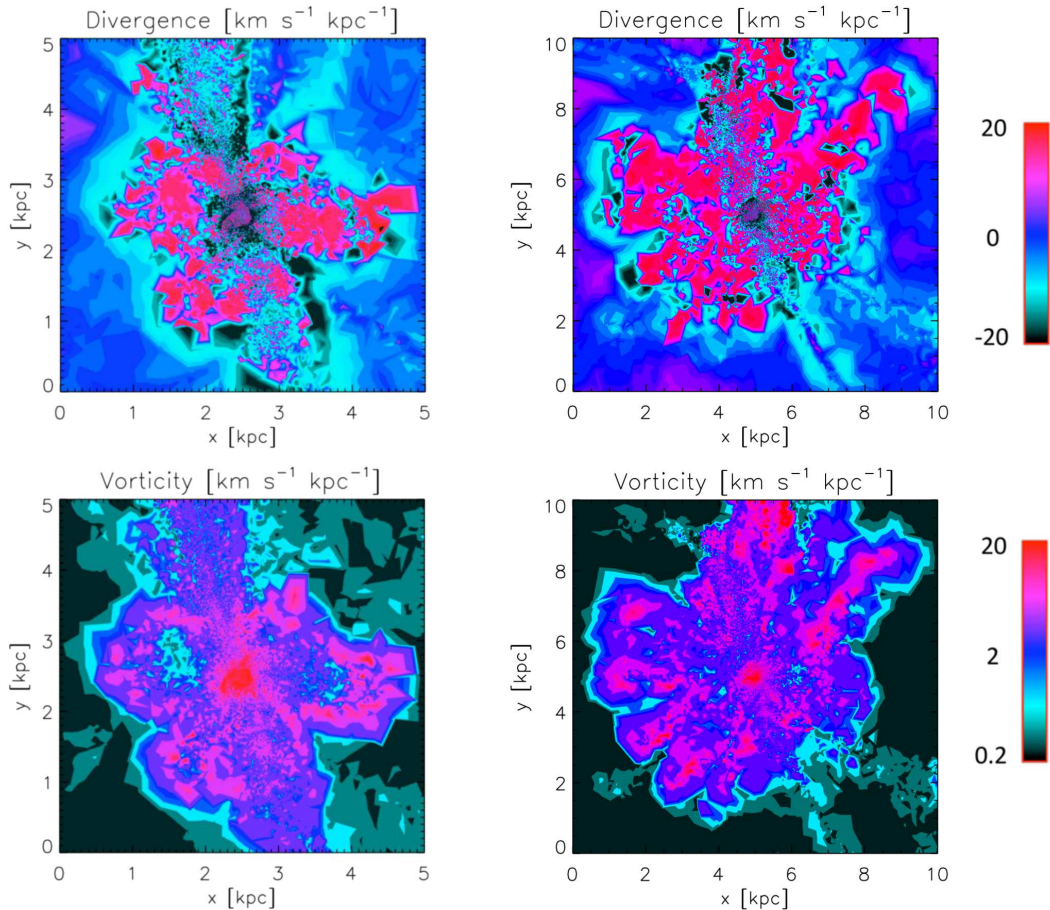


FIG. 7.— Divergence and vorticity in the protogalaxy due to supermassive explosions in dense regions (*left*) and diffuse H II regions (*right*). The divergence ( $|\nabla \cdot \vec{v}|$ , *top row*) marks regions of rapidly expanding flow and vorticity ( $|\nabla \times \vec{v}|$ , *bottom row*) traces shear flows that probably drive turbulence.

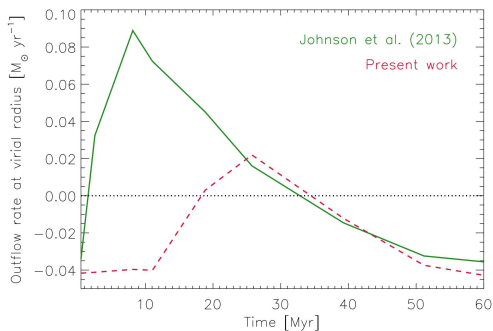


FIG. 8.— Outflow and fallback rates in the protogalaxy as a function of time for explosions in diffuse H II regions (*green line*) and dense regions (*red dashed line*).

Kilometer Array (SKA) at  $z \gtrsim 15$  (Mesler et al. 2012; Whalen et al. 2013d). In contrast to the NIR, this emission is much brighter for explosions in H II regions because of the higher shock temperatures and it has a profile that easily distinguishes it from less energetic Pop III SNe.

Later, on times of 10 - 20 Myr, fallback may activate emission by SMBH seeds in the halo that could be detected in the NIR by successors to *Swift* such as the Joint Astrophysics Nascent Universe Satellite (JANUS;

Roming 2008; Burrows et al. 2010), *Lobster*, or *EXIST*. At about this time chemical enrichment and cooling may also trigger starbursts that could be detected in the NIR by *JWST*, distinguishing these halos from their less luminous neighbors. Testing the prospects for rapid star formation and SMBH seed growth in line cooled halos after such explosions requires numerical simulations with metal and dust mixing and cooling together with x-ray feedback by the central BH that are now under development. We note that these explosions in principle could also be found in the CMB via the Sunyayev-Zel'dovich effect, but the likelier candidates for such detections are SNe in diffuse H II regions that enclose and upscatter greater numbers of CMB photons (e.g., Oh et al. 2003; Whalen et al. 2008).

The debris of these ancient explosions could also be found in the atmospheres of dim metal-poor stars in the Galactic halo today (e.g., Beers & Christlieb 2005; Frebel et al. 2005; Cayrel et al. 2004; Lai et al. 2008; Frebel & Bromm 2012). Gas enriched to the metallicities in our simulation is expected to fragment into stars  $\lesssim 0.8 M_{\odot}$  that may still exist, particularly if they formed in dust (Schneider et al. 2006). The chemical signatures of supermassive SNe can be distinguished from those of Pop III PI SNe because they create very little  $^{56}\text{Ni}$ , unlike PI SNe that produce iron-group elements (Heger & Woosley 2002). However, like PI SNe supermassive SNe make

few r-process and s-process elements, so their chemical fingerprint can also be differentiated from those of 15 - 40  $M_{\odot}$  Pop III core-collapse SNe. These abundance patterns may not have been detected yet because the stars that bear them were enriched to metallicities above those targeted by surveys of metal-poor stars to date (Karlsson et al. 2008) (see also Cooke et al. 2011; Ren et al. 2012, for tentative evidence of Pop III PI SNe in the fossil abundance record).

Besides marking the sites of formation of SMBHs on the sky, supermassive Pop III SNe would also reveal the location of their nurseries: line-cooled halos and the nearby protogalaxies that saturate them with strong LW fluxes (e.g., Dijkstra et al. 2008; Agarwal et al. 2012). These rapidly forming young galaxies could then be selected for spectroscopic followup by *JWST*. Detections of the most energetic thermonuclear explosions in the universe at  $z \gtrsim 15$  by the next generation of telescopes may finally reveal the origins of SMBHs.

We thank the anonymous referee, whose comments im-

proved the quality of this paper. JIJ and JS were supported by LANL LDRD Director's Fellowships. DJW acknowledges support from the Baden-Württemberg-Stiftung by contract research via the programme Internationale Spitzenforschung II (grant P-LS-SPII/18). AH was supported by the US DOE Program for Scientific Discovery through Advanced Computing (SciDAC; DE-FC02-09ER41618), by the US Department of Energy under grant DE-FG02-87ER40328, by the Joint Institute for Nuclear Astrophysics (JINA; NSF grant PHY08-22648 and PHY110-2511). AH also acknowledges support by an ARC Future Fellowship (FT120100363) and a Monash University Larkins Fellowship. Work at LANL was done under the auspices of the National Nuclear Security Administration of the U.S. Department of Energy at Los Alamos National Laboratory under Contract DE-AC52-06NA25396. All GADGET and ZEUS-MP simulations were performed on Institutional Computing platforms at LANL (Mustang and Pinto).

## REFERENCES

- Abel, T., Bryan, G. L., & Norman, M. L. 2000, *ApJ*, 540, 39  
— 2002, *Science*, 295, 93
- Abel, T., Wise, J. H., & Bryan, G. L. 2007, *ApJ*, 659, L87
- Agarwal, B., Khochfar, S., Johnson, J. L., Neistein, E., Dalla Vecchia, C., & Livio, M. 2012, *MNRAS*, 425, 2854
- Alvarez, M. A., Bromm, V., & Shapiro, P. R. 2006, *ApJ*, 639, 621
- Alvarez, M. A., Wise, J. H., & Abel, T. 2009, *ApJ*, 701, L133
- Appenzeller, I. & Fricke, K. 1972a, *A&A*, 18, 10  
— 1972b, *A&A*, 21, 285
- Beers, T. C. & Christlieb, N. 2005, *ARA&A*, 43, 531
- Begelman, M. C. 2010, *MNRAS*, 402, 673
- Begelman, M. C., Volonteri, M., & Rees, M. J. 2006, *MNRAS*, 370, 289
- Bond, J. R., Arnett, W. D., & Carr, B. J. 1984, *ApJ*, 280, 825
- Bromm, V., Coppi, P. S., & Larson, R. B. 1999, *ApJ*, 527, L5  
— 2002, *ApJ*, 564, 23
- Bromm, V., Ferrara, A., Coppi, P. S., & Larson, R. B. 2001, *MNRAS*, 328, 969
- Bromm, V. & Loeb, A. 2003, *ApJ*, 596, 34
- Burrows, D. N., Roming, P. W. A., Fox, D. B., Herter, T. L., Falcone, A., Bilén, S., Nousek, J. A., & Kennea, J. A. 2010, in Presented at the Society of Photo-Optical Instrumentation Engineers (SPIE) Conference, Vol. 7732, Society of Photo-Optical Instrumentation Engineers (SPIE) Conference Series
- Cayrel, R., Depagne, E., Spite, M., Hill, V., Spite, F., François, P., Plez, B., Beers, T., Primas, F., Andersen, J., Barbuy, B., Bonifacio, P., Molaro, P., & Nordström, B. 2004, *A&A*, 416, 1117
- Cherchneff, I. & Dwek, E. 2009, *ApJ*, 703, 642  
— 2010, *ApJ*, 713, 1
- Cherchneff, I. & Lilly, S. 2008, *ApJ*, 683, L123
- Chiaki, G., Yoshida, N., & Kitayama, T. 2013, *ApJ*, 762, 50
- Choi, J.-H., Shlosman, I., & Begelman, M. C. 2013, *ApJ*, 774, 149
- Clark, P. C., Glover, S. C. O., Smith, R. J., Greif, T. H., Klessen, R. S., & Bromm, V. 2011, *Science*, 331, 1040
- Cooke, R., Pettini, M., Steidel, C. C., Rudie, G. C., & Jorgenson, R. A. 2011, *MNRAS*, 412, 1047
- de Souza, R. S., Ishida, E. E. O., Johnson, J. L., Whalen, D. J., & Mesinger, A. 2013, arXiv:1306.4984
- de Souza, R. S., Rodrigues, L. F. S., Ishida, E. E. O., & Opher, R. 2011, *MNRAS*, 415, 2969
- Dessart, L., Waldman, R., Livne, E., Hillier, D. J., & Blondin, S. 2013, *MNRAS*, 428, 3227
- Dijkstra, M., Haiman, Z., Mesinger, A., & Wyithe, J. S. B. 2008, *MNRAS*, 391, 1961
- Djorgovski, S. G., Volonteri, M., Springel, V., Bromm, V., & Meylan, G. 2008, in The Eleventh Marcel Grossmann Meeting On Recent Developments in Theoretical and Experimental General Relativity, Gravitation and Relativistic Field Theories, ed. H. Kleinert, R. T. Jantzen, & R. Ruffini, 340–367
- Dwek, E. & Cherchneff, I. 2011, *ApJ*, 727, 63
- Fan, X., Strauss, M. A., Richards, G. T., Hennawi, J. F., Becker, R. H., White, R. L., Diamond-Stanic, A. M., Donley, J. L., Jiang, L., Kim, J. S., Vestergaard, M., Young, J. E., Gunn, J. E., Lupton, R. H., Knapp, G. R., Schneider, D. P., Brandt, W. N., Bahcall, N. A., Barentine, J. C., Brinkmann, J., Brewington, H. J., Fukugita, M., Harvanek, M., Kleinman, S. J., Krzesinski, J., Long, D., Neilsen, Jr., E. H., Nitta, A., Snedden, S. A., & Voges, W. 2006, *AJ*, 131, 1203
- Fan, X., Strauss, M. A., Schneider, D. P., Becker, R. H., White, R. L., Haiman, Z., Gregg, M., Pentericci, L., Grebel, E. K., Narayanan, V. K., Loh, Y., Richards, G. T., Gunn, J. E., Lupton, R. H., Knapp, G. R., Ivezić, Ž., Brandt, W. N., Collinge, M., Hao, L., Harbeck, D., Prada, F., Schaye, J., Strateva, I., Zakamska, N., Anderson, S., Brinkmann, J., Bahcall, N. A., Lamb, D. Q., Okamura, S., Szalay, A., & York, D. G. 2003, *AJ*, 125, 1649
- Fowler, W. A. 1966, *ApJ*, 144, 180
- Fowler, W. A. & Hoyle, F. 1964, *ApJS*, 9, 201
- Frebel, A., Aoki, W., Christlieb, N., Ando, H., Asplund, M., Barklem, P. S., Beers, T. C., Eriksson, K., Fechner, C., Fujimoto, M. Y., Honda, S., Kajino, T., Minezaki, T., Nomoto, K., Norris, J. E., Ryan, S. G., Takada-Hidai, M., Tsangarides, S., & Yoshii, Y. 2005, *Nature*, 434, 871
- Frebel, A. & Bromm, V. 2012, *ApJ*, 759, 115
- Frey, L. H., Even, W., Whalen, D. J., Fryer, C. L., Hungerford, A. L., Fontes, C. J., & Colgan, J. 2013, *ApJS*, 204, 16
- Fryer, C. L., Whalen, D. J., & Frey, L. 2010, in American Institute of Physics Conference Series, Vol. 1294, American Institute of Physics Conference Series, ed. D. J. Whalen, V. Bromm, & N. Yoshida, 70–75
- Fuller, G. M., Woosley, S. E., & Weaver, T. A. 1986, *ApJ*, 307, 675
- Gall, C., Hjorth, J., & Andersen, A. C. 2011, *A&A Rev.*, 19, 43
- Gittings, M., Weaver, R., Clover, M., Betlach, T., Byrne, N., Coker, R., Dendy, E., Hueckstaedt, R., New, K., Oakes, W. R., Ranta, D., & Stefan, R. 2008, *Computational Science and Discovery*, 1, 015005
- Greif, T. H., Bromm, V., Clark, P. C., Glover, S. C. O., Smith, R. J., Klessen, R. S., Yoshida, N., & Springel, V. 2012, *MNRAS*, 424, 399
- Greif, T. H., Glover, S. C. O., Bromm, V., & Klessen, R. S. 2010, *ApJ*, 716, 510

- Greif, T. H., Johnson, J. L., Klessen, R. S., & Bromm, V. 2008, *MNRAS*, 387, 1021
- Greif, T. H., Springel, V., White, S. D. M., Glover, S. C. O., Clark, P. C., Smith, R. J., Klessen, R. S., & Bromm, V. 2011, *ApJ*, 737, 75
- Heger, A. & Chen, K.-J. 2013, *ApJ*, in prep
- Heger, A. & Woosley, S. E. 2002, *ApJ*, 567, 532
- Hosokawa, T., Omukai, K., Yoshida, N., & Yorke, H. W. 2011, *Science*, 334, 1250
- Hummel, J. A., Pawlik, A. H., Milosavljević, M., & Bromm, V. 2012, *ApJ*, 755, 72
- Iben, Jr., I. 1963, *ApJ*, 138, 1090
- Jeon, M., Pawlik, A. H., Greif, T. H., Glover, S. C. O., Bromm, V., Milosavljević, M., & Klessen, R. S. 2012, *ApJ*, 754, 34
- Joggerst, C. C., Almgren, A., Bell, J., Heger, A., Whalen, D., & Woosley, S. E. 2010, *ApJ*, 709, 11
- Joggerst, C. C. & Whalen, D. J. 2011, *ApJ*, 728, 129
- Johnson, J. L. & Bromm, V. 2006, *MNRAS*, 366, 247
- , 2007, *MNRAS*, 374, 1557
- Johnson, J. L., Greif, T. H., & Bromm, V. 2008, *MNRAS*, 388, 26
- Johnson, J. L., Greif, T. H., Bromm, V., Klessen, R. S., & Ippolito, J. 2009, *MNRAS*, 399, 37
- Johnson, J. L., Khochfar, S., Greif, T. H., & Durier, F. 2011, *MNRAS*, 410, 919
- Johnson, J. L., Whalen, D. J., Even, W., Fryer, C. L., Heger, A., Smidt, J., & Chen, K.-J. 2013a, arXiv:1304.4601
- Johnson, J. L., Whalen, D. J., Fryer, C. L., & Li, H. 2012, *ApJ*, 750, 66
- Johnson, J. L., Whalen, D. J., Li, H., & Holz, D. E. 2013b, *ApJ*, 771, 116
- Karlsson, T., Johnson, J. L., & Bromm, V. 2008, *ApJ*, 679, 6
- Kasen, D., Woosley, S. E., & Heger, A. 2011, *ApJ*, 734, 102
- Kitayama, T. & Yoshida, N. 2005, *ApJ*, 630, 675
- Kitayama, T., Yoshida, N., Susa, H., & Umemura, M. 2004, *ApJ*, 613, 631
- Lai, D. K., Bolte, M., Johnson, J. A., Lucatello, S., Heger, A., & Woosley, S. E. 2008, *ApJ*, 681, 1524
- Latif, M. A., Schleicher, D. R. G., Schmidt, W., & Niemeyer, J. 2013a, *MNRAS*, 433, 1607
- , 2013b, *MNRAS*, 430, 588
- Lippai, Z., Frei, Z., & Haiman, Z. 2009, *ApJ*, 701, 360
- Mackey, J., Bromm, V., & Hernquist, L. 2003, *ApJ*, 586, 1
- Meiksin, A. & Whalen, D. J. 2013, *MNRAS*, 430, 2854
- Mesler, R. A., Whalen, D. J., Lloyd-Ronning, N. M., Fryer, C. L., & Pihlström, Y. M. 2012, *ApJ*, 757, 117
- Milosavljević, M., Bromm, V., Couch, S. M., & Oh, S. P. 2009, *ApJ*, 698, 766
- Montero, P. J., Janka, H.-T., & Müller, E. 2012, *ApJ*, 749, 37
- Mortlock, D. J., Warren, S. J., Venemans, B. P., Patel, M., Hewett, P. C., McMahon, R. G., Simpson, C., Theuns, T., González-Solares, E. A., Adamson, A., Dye, S., Hambly, N. C., Hirst, P., Irwin, M. J., Kuiper, E., Lawrence, A., & Röttgering, H. J. A. 2011, *Nature*, 474, 616
- Nakamura, F. & Umemura, M. 2001, *ApJ*, 548, 19
- Oh, S. P., Cooray, A., & Kamionkowski, M. 2003, *MNRAS*, 342, L20
- Omukai, K., Schneider, R., & Haiman, Z. 2008, *ApJ*, 686, 801
- O’Shea, B. W. & Norman, M. L. 2007, *ApJ*, 654, 66
- , 2008, *ApJ*, 673, 14
- Pan, T., Kasen, D., & Loeb, A. 2012a, *MNRAS*, 422, 2701
- Pan, T., Loeb, A., & Kasen, D. 2012b, *MNRAS*, 423, 2203
- Park, K. & Ricotti, M. 2011, *ApJ*, 739, 2
- , 2012, *ApJ*, 747, 9
- , 2013, *ApJ*, 767, 163
- Pawlik, A. H., Milosavljević, M., & Bromm, V. 2011, *ApJ*, 731, 54
- , 2013, *ApJ*, 767, 59
- Petri, A., Ferrara, A., & Salvaterra, R. 2012, *MNRAS*, 422, 1690
- Regan, J. A. & Haehnelt, M. G. 2009, *MNRAS*, 396, 343
- Ren, J., Christlieb, N., & Zhao, G. 2012, *Research in Astronomy and Astrophysics*, 12, 1637
- Ritter, J. S., Safranek-Shrader, C., Gnat, O., Milosavljević, M., & Bromm, V. 2012, *ApJ*, 761, 56
- Roming, P. 2008, in *COSPAR, Plenary Meeting*, Vol. 37, 37th COSPAR Scientific Assembly, 2645–+
- Safranek-Shrader, C., Milosavljevic, M., & Bromm, V. 2013, arXiv:1307.1982
- Santoro, F. & Shull, J. M. 2006, *ApJ*, 643, 26
- Scannapieco, E., Madau, P., Woosley, S., Heger, A., & Ferrara, A. 2005, *ApJ*, 633, 1031
- Schleicher, D. R. G., Palla, F., Ferrara, A., Galli, D., & Latif, M. 2013, arXiv:1305.5923
- Schneider, R., Omukai, K., Inoue, A. K., & Ferrara, A. 2006, *MNRAS*, 369, 1437
- Shang, C., Bryan, G. L., & Haiman, Z. 2010, *MNRAS*, 402, 1249
- Smith, B. D. & Sigurdsson, S. 2007, *ApJ*, 661, L5
- Smith, B. D., Turk, M. J., Sigurdsson, S., O’Shea, B. W., & Norman, M. L. 2009, *ApJ*, 691, 441
- Smith, R. J., Glover, S. C. O., Clark, P. C., Greif, T., & Klessen, R. S. 2011, *MNRAS*, 414, 3633
- Springel, V. & Hernquist, L. 2002, *MNRAS*, 333, 649
- Springel, V., Yoshida, N., & White, S. D. M. 2001, *New Astronomy*, 6, 79
- Stacy, A., Greif, T. H., & Bromm, V. 2010, *MNRAS*, 403, 45
- Susa, H. 2013, *ApJ*, 773, 185
- Tanaka, T. & Haiman, Z. 2009, *ApJ*, 696, 1798
- Turk, M. J., Abel, T., & O’Shea, B. 2009, *Science*, 325, 601
- Vasiliev, E. O., Vorobyov, E. I., Matvienko, E. E., Razoumov, A. O., & Shchekinov, Y. A. 2012, *Astronomy Reports*, 56, 895
- Weaver, T. A., Zimmerman, G. B., & Woosley, S. E. 1978, *ApJ*, 225, 1021
- Whalen, D., Abel, T., & Norman, M. L. 2004, *ApJ*, 610, 14
- Whalen, D. & Norman, M. L. 2006, *ApJS*, 162, 281
- , 2008a, *ApJ*, 673, 664
- Whalen, D., van Veelen, B., O’Shea, B. W., & Norman, M. L. 2008, *ApJ*, 682, 49
- Whalen, D. J., Even, W., Frey, L. H., Johnson, J. L., Lovekin, C. C., Fryer, C. L., Stiavelli, M., Holz, D. E., Heger, A., Woosley, S. E., & Hungerford, A. L. 2012a, arXiv:1211.4979
- Whalen, D. J., Even, W., Lovekin, C. C., Fryer, C. L., Stiavelli, M., Roming, P. W. A., Cooke, J., Pritchard, T. A., Holz, D. E., & Knight, C. 2013a, *ApJ*, 768, 195
- Whalen, D. J. & Fryer, C. L. 2012, *ApJ*, 756, L19
- Whalen, D. J., Fryer, C. L., Holz, D. E., Heger, A., Woosley, S. E., Stiavelli, M., Even, W., & Frey, L. H. 2013b, *ApJ*, 762, L6
- Whalen, D. J., Heger, A., Chen, K.-J., Even, W., Fryer, C. L., Stiavelli, M., Xu, H., & Joggerst, C. C. 2012b, arXiv:1211.1815
- Whalen, D. J., Joggerst, C. C., Fryer, C. L., Stiavelli, M., Heger, A., & Holz, D. E. 2013c, *ApJ*, 768, 95
- Whalen, D. J., Johnson, J. J., Smidt, J., Meiksin, A., Heger, A., Even, W., & Fryer, C. L. 2013d, arXiv:1305.6966
- Whalen, D. J. & Norman, M. L. 2008b, *ApJ*, 672, 287
- Willott, C. J., McLure, R. J., & Jarvis, M. J. 2003, *ApJ*, 587, L15
- Wise, J. H. & Abel, T. 2007, *ApJ*, 671, 1559
- , 2008, *ApJ*, 684, 1
- Wise, J. H., Turk, M. J., & Abel, T. 2008, *ApJ*, 682, 745
- Wise, J. H., Turk, M. J., Norman, M. L., & Abel, T. 2012, *ApJ*, 745, 50
- Wolcott-Green, J., Haiman, Z., & Bryan, G. L. 2011, *MNRAS*, 418, 838
- Woosley, S. E., Heger, A., & Weaver, T. A. 2002, *Reviews of Modern Physics*, 74, 1015
- Yoshida, N., Omukai, K., & Hernquist, L. 2008, *Science*, 321, 669